Conformational Behavior of Giant DNA through Binding with Ag^+ and Metallization

Anatoly A. Zinchenko,*[,†,‡] Damien Baigl,[‡,§] Ning Chen,[†,‡] Olga Pyshkina,[||] Kazunaka Endo,[⊥] Vladimir G. Sergeyev,[||] and Kenichi Yoshikawa[‡,#]

Graduate School of Environmental Studies, Nagoya University, Chikusa, Furo, Nagoya 464-8601, Japan, Spatio-Temporal Order Project, ICORP, JST, Japan, Department of Physics, Kyoto University, Sakyo, Kyoto, 608-8501, Japan, Department of Chemistry, Ecole Normale Supérieure, Paris F-75005, France, Department of Polymer Science, Faculty of Chemistry, Moscow State University, Moscow, 119899, Russia, Graduate School of Natural Science and Technology, Kanazawa University, Kakuma, Kanazawa 9201192, Japan

Received March 3, 2008; Revised Manuscript Received May 1, 2008

The conformational behavior of a long single-chain double-stranded DNA in solutions of free silver ions and silver nanoparticles generated via the reduction of $AgNO_3$ by $NaBH_4$ was monitored by fluorescence and electron microscopies and UV spectroscopy. The interaction of monovalent silver ions with DNA induces shrinking of a DNA-coiled polymer chain as a result of a decrease in the DNA persistence length through the complexation of Ag^+ with DNA bases. In contrast, the reduction of silver ions by $NaBH_4$ in DNA solutions triggers DNA compaction: a DNA transition from elongated coil state into a compact state. This transition is continuous, unlike the all-or-none discrete DNA compaction that is commonly seen with multications. It is suggested that the collapse of DNA is accompanied by growth aggregation of silver nanoparticles generated on the DNA template.

Introduction

Investigations on DNA interaction with Ag^+ and other transition metal ions, such as Hg^{2+}, Au^+, Cu^{2+}, and so on, started right after the DNA double helix was discovered.[1,2] These earliest reports described DNA interactions with transition metal ions (M^+) at up to equimolar ratios (M^+ to DNA phosphates) by conventional spectroscopic, electrochemical, and other physicochemical techniques.[3] It is now recognized that Ag^+ ions prefer coordinating with DNA bases to electrostatic binding with DNA phosphates[4] and such coordination with DNA bases has three modes of binding.[5] At Ag/nucleotide ratios below 0.2, the type I complex is formed with the guanine N7 atom as a major binding site, whereas at ratios of 0.2−0.5, type II complexes are formed with A−T or G−C base pairs as main binding targets. Finally, at ratios above 0.5, type III complexes are formed when the major binding sites in type I and type II complexes are saturated.

Since that time, the investigation of DNA−silver interactions has been virtually suspended right up to recent intensive studies in the fields of nanoscale chemistry, biophysics, and biomaterials. The rapid development of new synthetic approaches in the area of metal nanostructure preparation has stimulated new scientific interest in the interaction between biological macromolecules, such as DNA or proteins, and metal nanostructures, which are remarkable for their outstanding electronic and optical properties[6] and promising for future applications in bioimaging, nanoelectronics, sensor preparation, and so on. It has been shown that the reduction of noble metal ions in the presence of a polyelectrolyte scaffold leads to the deposition of metal in the form of nanoparticles in a DNA template to form nanowires.[7] In these experiments, DNA was usually fixed onto a solid substrate prior to the deposition of metals on DNA and, therefore, the conformational properties of a DNA chain in bulk were not revealed. However, the conformation of a DNA molecule is an important property that not only determines the behavior of DNA in solution but is also closely interrelated with the biological activity of DNA.[8] Furthermore, an understanding of the DNA conformational response to DNA scaffold metallization should provide deeper insight into the forces that play a role in DNA metallization. In the current report, we discuss the conformational behavior of a long DNA (bacteriophage T4) in a solution of silver ions and silver nanoparticles formed by Ag^+ reduction. We show that metallization of DNA by silver cations leads to the reduction of DNA persistent length, while metallization of DNA by silver nanoparticles induces DNA compaction.

Experimental Section

Materials. Bacteriophage T4 DNA (166000 base pairs, Nippon Gene Co., LTD, Japan), $AgNO_3$ (99.9999% purity, Aldrich, Japan), the fluorescent dye YOYO-1 (1,1′-(4,4,7,7-tetramethyl-4,7-diazaundecamethylene)-bis-4-[3-methyl-2,3-dihydro-(benzo-1,3-oxazole)-2-methylidene]-quinolinium tetraiodide) (Molecular Probes, U.S.A.), and sodium borohydride, $NaBH_4$ (Nacalai Tesque Inc., Japan), were used for this study.

Fluorescence Microscopy (FM). Fluorescence images of individual DNA molecules were observed using a Zeiss Axiovert 135 TV microscope equipped with a 100 × oil-immersed lens and recorded on S-VHS videotapes through a Hamamatsu SIT TV camera.

UV−vis Spectroscopy. UV−vis spectra were recorded on a Jasco U-550 UV/vis spectrophotometer in 1.0 × 0.2 × 0.5 cm quartz cells.

Electron Microscopy. Transmission electron microscopic (TEM) observations were performed at room temperature using a JEM-1200EX

* To whom correspondence should be addressed. E-mail: zinchenko@urban.env.nagoya-u.ac.jp.
† Nagoya University.
‡ ICORP.
§ Ecole Normale Supérieure.
|| Moscow State University.
⊥ Kanazawa University.
Kyoto University.

10.1021/bm800235j CCC: $40.75
Published on Web 06/25/2008

microscope (JEOL) at an acceleration voltage of 100 kV using 300 mesh carbon-coated grids. Silver nanoparticles were observed without staining. For DNA observation, uranyl acetate (1 wt % in water) was used as a staining agent.

Sample Solutions. Special precautions were taken to prevent the silver ion complexation, reduction, or precipitation by the chemicals used for sample preparation. For this purpose, DNA solutions were prepared in Milli-Q water without salt or buffer. Because concentrated T4 DNA stock (1 mM) is available commercially as a buffer solution (10 mM Tris-HCl (pH 7.5) and 1 mM EDTA), after dilution, T4 DNA sample solutions always contained small amounts of EDTA and Tris-HCl. Certainly, EDTA and Cl^- ions are able to interact with silver ions, however, according to the stability constants,[9] the complexation of Ag^+ with EDTA or interaction with Cl^- is negligible compared to reduction by $NaBH_4$. Moreover, removal of all buffer components from the solution would be critical for DNA molecule stability. It should be also mentioned that YOYO is an iodide salt, therefore, I^- can bind to Ag^+, but because the concentration of YOYO is always five times lower than the concentration of DNA in microscopy experiments, we neglect its influence in the experiments.

Samples for FM and UV spectroscopy measurements were prepared as follows. First, a stock solution containing T4 DNA (10^{-6} M) and YOYO (2×10^{-7} M) was prepared in Milli-Q water. Final sample solutions for UV or FM investigations were then made by a 100-fold dilution of the stock solution (i.e., final concentration of T4 DNA was 10^{-8} M) and addition of the necessary amounts of $AgNO_3$ and $NaBH_4$. The samples were observed by FM after an additional 30 min. Solutions with a DNA concentration of 10^{-7} M were prepared in a similar manner.

Solutions for electron microscopic observations contained 10^{-6} M of T4 DNA in Milli-Q water and appropriate concentrations of $AgNO_3$ and $NaBH_4$.

Results and Discussion

Conformational Behavior of DNA in $AgNO_3$ Solutions. To investigate the effect of silver ions on the conformational behavior of individual DNA molecules, FM observations were carried out in real time in aqueous diluted solutions of YOYO-labeled T4 DNA (166000 bp, 10^{-8} M) in the presence of $AgNO_3$. Typical fluorescence images of T4 DNA molecules with an increase in the $AgNO_3$ concentration are shown in Figure 1A. Up to a $AgNO_3$ concentration of 10^{-6} M, all DNA molecules remained in an unfolded coil state. However, a further increase in the $AgNO_3$ concentration induced a gradual and significant shrinking of individual DNA molecules. Finally, at a $AgNO_3$ concentration above 10^{-4} M, the image of T4 DNA vanished completely. Changes in the DNA fluorescent image is attributed to the binding of Ag^+ ions to the heteroatoms of nucleic bases.[10] Upon such binding, DNA bases are twisted or tilted, which converts DNA base pairs from a perpendicular to a propeller arrangement with respect to the axis of the DNA helix.[11] The change in the base-pair twist angle considerably weakens the strength of binding between YOYO and DNA bases, which leads to the further release of dye molecules from the double helix. As a result, the image of T4 DNA vanished at higher Ag^+ concentrations.

To characterize changes in the conformation of DNA in a DNA−Ag complex in a quantitative manner, FM observations were carried out by varying the concentration of silver ions from 10^{-9} to 10^{-4} M. The dependence of the average long-axis length (longer distance in the outline of DNA molecular fluorescence image) of T4 DNA at various $AgNO_3$ concentrations is shown in Figure 1B. It shows that, when the concentration of Ag^+ is lower than 10^{-6} M, the maximum of the DNA coil size distribution is around 3 μm and the distribution is rather wide,

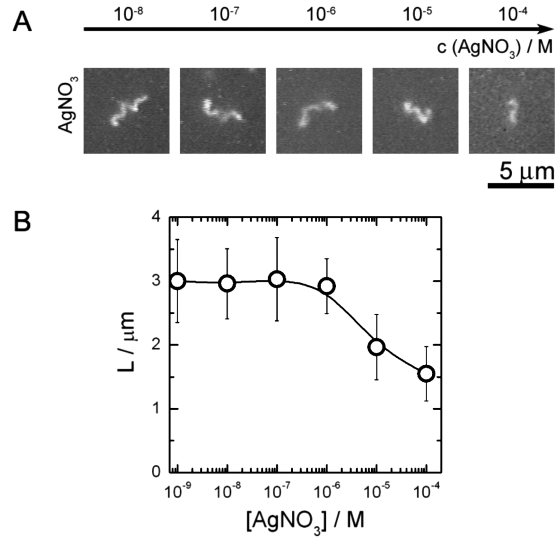

Figure 1. (A) Fluorescence microscopy (FM) images of T4 DNA molecules at different concentrations of $AgNO_3$ in aqueous solution. Solutions were prepared by mixing $AgNO_3$ solution with a DNA solution (10^{-8} M). (B) Dependence of the long-axis length, *L*, of individual T4-DNA molecules (averaged over ca. 100 molecules) on the $AgNO_3$ concentration. Symbols on the plot indicate the maximums of length distributions; the width of the distribution is given as a standard deviation.

indicating that DNA exists in an elongated coil state. A further increase in the Ag^+ concentration causes a decrease in the DNA effective length, and when the Ag^+ concentration is about 10^{-4} M, the maximum of the DNA length distribution is around 1.5 μm; that is, DNA is about 2-fold smaller than in the original coil state but still exhibits large intramolecular fluctuations, which are characteristic of a shrunken coil state. This suggests that the persistence length is reduced by about half, because the DNA long-axis length is proportional to the DNA persistence length for sufficiently long DNA molecules. It is now clear that silver ions contribute to the shrinking of DNA molecules through interaction with Ag^+ ions. It should be noted that due to the possible interaction of Ag^+ with EDTA and the Cl^- ion coming from Tris buffer, at concentrations of Ag^+ up to 10^{-7} M, the effects of Ag^+ ions can be partly inactivated due to the interaction with such buffer components.

It is known that Ag^+ has an electronic configuration that favors the formation of strong complexes with DNA bases.[5] As a consequence, a positive charge is introduced inside the negatively charged DNA double helix. Due to the presence of positive charges along the chain, there is a marked decrease in the external electric field. Perturbations in the charge distribution could be primarily responsible for the decrease in length because of the reduction in the net electrostatic repulsive forces along the DNA helix. Therefore, the rearrangement of DNA bases together with the reduction of electrostatic repulsive forces induced by Ag^+ complexation with DNA might contribute to the significant decrease in DNA persistence length. In addition to purely electrostatic reasons for DNA shrinking, one can also consider binding of at least a two-coordinate silver cation with different sites along a DNA chain and possible photochemical reduction of silver mediated by DNA organic groups.

Our FM observations show direct microscopic evidence of the changes in the DNA effective volume upon complexation with Ag^+. It should be noted that the binding site of Ag^+ to DNA is different from that of alkali ions such as Na^+ or K^+, which act mainly as counterions, whereas heavy metal ions intercalate inside the DNA double helix. Therefore, the effect

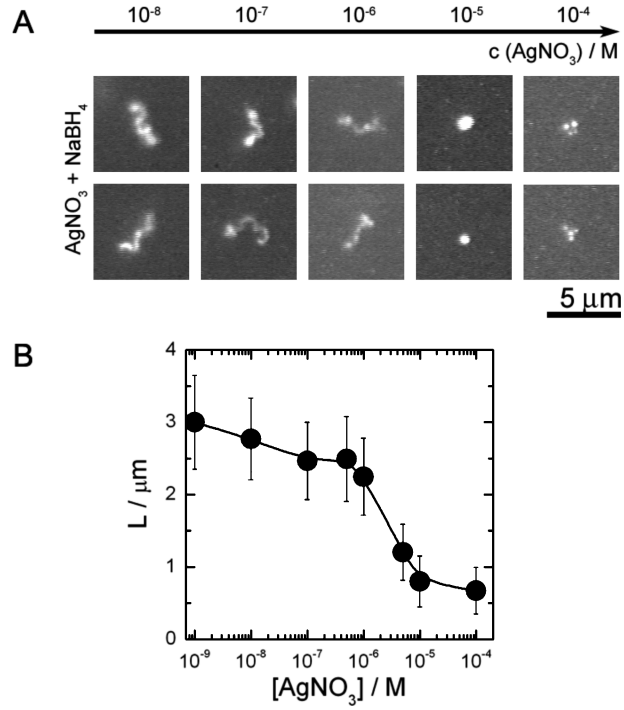

Figure 2. (A) Fluorescence images of T4 DNA molecules at different concentrations of $AgNO_3$ and $NaBH_4$ (reducing agent). Solutions were prepared by mixing $AgNO_3$ solution with a DNA solution (10^{-8} M) and the further addition of a 10-fold excess of $NaBH_4$ (for each $AgNO_3$ concentrations, two images are shown for better illustration). (B) Dependence of the long-axis length (*L*) of individual T4-DNA molecules (averaged over ca. 100 molecules) on the $AgNO_3$ concentration in the presence of a 10-fold excess of $NaBH_4$ to $AgNO_3$. Symbols on the plot indicate the maximums of length distributions; the width of the distribution is given as a standard deviation.

of the Ag^+ ion on the DNA conformation is substantially different from that of alkali cations, where a comparable decrease in the effective size of DNA is observed at 100- to 1000-fold higher concentrations than in the case of Ag^+.[12]

Our further goal was to monitor changes in the conformation of DNA after metallization of the DNA chain when the silver ion is reduced to a neutral atom. The incorporation of Ag^+ ions into a DNA helix may contribute to the construction of functionalized nanomaterials, such as molecular wires, based on the deposition of metal nanoparticles on a DNA chain. As a basic method, silver nanostructure formation can be achieved by the chemical reduction of silver ions.

Formation of Silver Nanoparticles Triggers T4 DNA Compaction. It is known that reduction of Ag^+ ions in aqueous solution of sodium borohydride in the presence of polyphosphates leads to the formation of long-lived silver clusters besides particles of metallic silver.[13] The stabilization of the clusters and particles is brought about by polyanion being present at low concentration. Therefore, we could expect that native DNA as well as polyphosphate molecules can play an important role in the stabilization of clusters and particles formed upon reduction of silver ions by sodium borohydride in aqueous solution. To make a clear interaction between DNA and silver nanoparticles, two sets of preliminary experiments had to be done using silver ions and its mixture with DNA upon titration by sodium borohydride.

To ensure that all of the Ag^+ ions are reduced, all experiments were conducted at various DNA and silver nitrate concentrations but at a constant molar ratio of borohydride to silver equal to 10. Figure 2A shows typical fluorescence images of a T4 DNA upon the reduction of silver ions by sodium borohydride in DNA solution. The conformational behavior of DNA below $[AgNO_3] = 10^{-6}$ M is very similar to that when no reducing agent is added (Figure 1A); DNA exists in an elongated coil conformation with a characteristic long-axis length of 3 μm. However, formation of larger amounts of nanoparticles at higher concentrations of $AgNO_3$ and $NaBH_4$ leads to pronounced DNA conformational changes. At $[AgNO_3] = 5 \times 10^{-6}$ M, the DNA length drastically decreases, while the brightness of the DNA fluorescent images increases. At $[AgNO_3] = 10^{-5}$ M, highly shrunken, bright DNA images were observed together with a significant fraction of individual compact globules. The compact DNA globules did not aggregate nor precipitate on the microscope glass slide. This colloidal stability is attributed to a remaining charge of the compact globules. Finally, at $[AgNO_3] = 10^{-4}$ M, all DNA molecules were in a globule state, partly in the form of multiglobular aggregates. Such aggregates are supposed to be formed due to the capture of individual DNA globules into aggregates of a large number of nanoparticles. Because there was no stabilizer used in the experiments, after preparation, DNA−metal complexes slowly aggregated and formed larger condensates.

The change in the T4 DNA long-axis length averaged over about 100 individual DNA molecules is shown in Figure 2B as a function of $AgNO_3$ concentration. Despite the similarity in shape (Figures 1 and 2), the reduction of $AgNO_3$ with $NaBH_4$ induces complete DNA compaction into globules, while in the presence of $AgNO_3$ alone, DNA molecules shrink but remain in a coil state.

As mentioned above, the addition of $AgNO_3$ to DNA solution quenches the fluorescence image of a DNA chain. In contrast, the fact that DNA fluorescence images were clearly observed at a higher concentration of reduced $AgNO_3$ in solution indicates that a reduction of silver ions may decrease the amount of Ag^+ bound to the DNA helix due to the shift in the equilibrium of the reaction

$$Ag^+ + DNA \rightarrow [DNA - Ag]^+ \quad (1)$$

to the left, which would favor the intercalation of YOYO into the DNA helix.

Because a reduction of the Ag^+ ion under appropriate conditions leads to the formation of silver nanoparticles,[14] we can hypothesize that T4 DNA compaction is mediated by the formation of silver nanoparticles. UV−vis spectroscopy is a useful tool for monitoring the formation of silver nanoparticles. Due to the high UV−vis absorbance of silver nanoparticles, we were able to investigate the DNA/$AgNO_3$/$NaBH_4$ system under exactly the same conditions as were used for the FM observations and could compare the results of FM and UV−vis spectroscopy. UV spectra of DNA/$AgNO_3$/$NaBH_4$ solutions with various concentrations of silver nitrate are shown in Figure 3.

Solutions with and without DNA showed similar trends in UV−vis spectra upon the reduction of Ag^+ ion. At low concentrations of $AgNO_3$ (10^{-8} M), the solution showed very weak absorbance with no marked peaks. An adsorption peak appeared near 400 nm beginning at a $AgNO_3$ concentration of 5×10^{-7} M. Considerable spectral changes were accompanied by visual changes in the color of the solutions from $[AgNO_3] = 5 \times 10^{-6}$ M. The solution turned yellow and the intensity of this yellow color progressively increased. At the same time, the intensities of the peak at about 400 nm and a shoulder at about 250 nm increased dramatically. The appearance of a silver surface plasmon peak at around 400 nm clearly indicates the formation of silver nanoparticles within the range of 5−15 nm.[15]

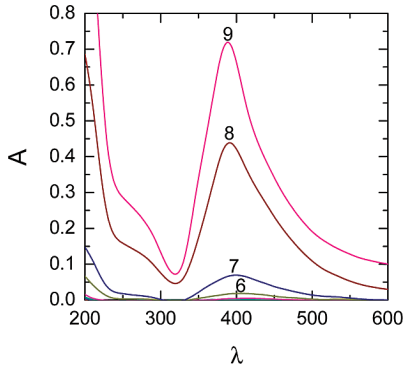

Figure 3. UV−vis absorbance spectra of a DNA/$AgNO_3$/$NaBH_4$ system at various concentrations of $AgNO_3$/$NaBH_4$. Solutions were prepared by the addition of $AgNO_3$ (1, 10^{-8} M; 2, 5×10^{-8} M; 3, 10^{-7} M; 4, 5×10^{-7} M; 5, 10^{-6} M; 6, 5×10^{-6} M; 7, 10^{-5} M; 8, 5×10^{-5} M; 9, 10^{-4} M) to the DNA solution (10^{-8} M) and further reduction by $NaBH_4$ (10-fold excess to $AgNO_3$). Curves 1−5 exhibit no detectible peaks. Experimental conditions are identical to those used for FM observations.

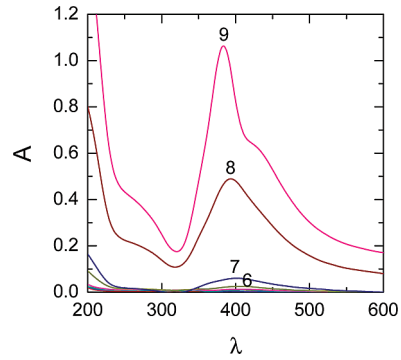

Figure 4. UV−vis absorbance spectra of $AgNO_3$/$NaBH_4$ system at various concentrations of $AgNO_3$/$NaBH_4$. Solutions were prepared by the reduction of $AgNO_3$ (1,10^{-8} M; 2, 5×10^{-8} M; 3, 10^{-7} M; 4, 5×10^{-7} M; 5, 10^{-6} M; 6, 5×10^{-6} M; 7, 10^{-5} M; 8, 5×10^{-5} M; 9, 10^{-4} M) by $NaBH_4$ (10-fold excess to $AgNO_3$). Curves 1−5 exhibit no detectible peaks.

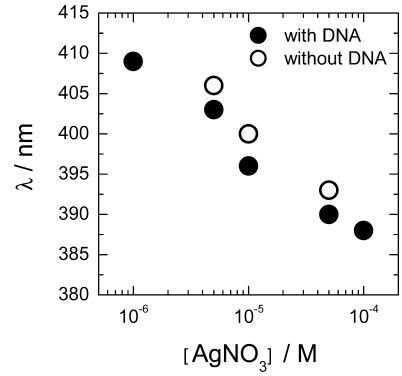

Figure 5. Dependence of UV−vis absorbance maximum of DNA/$AgNO_3$/$NaBH_4$ (●) and $AgNO_3$/$NaBH_4$ (○) systems on the concentrations of $AgNO_3$. Experimental points were taken from the analysis of UV−vis experimental results in Figures 3 and 4.

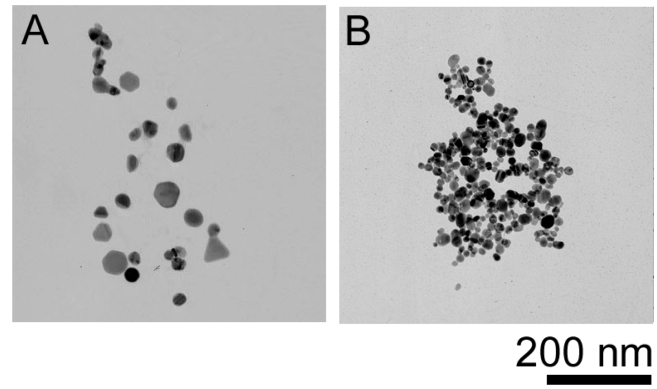

Figure 6. Transmission electron microscopic images of silver nanoparticles observed after reduction of $AgNO_3$ with $NaBH_4$. Concentrations of $AgNO_3$ are 10^{-5} M (A) and 10^{-4} M (B), respectively.

It is well-known that the wavelength of surface plasmon of silver nanoparticles provides information about the size of the nanoparticles. This increase in the size of silver nanoparticles corresponds to the red shift of the absorbance maximum.[16] In our experiments, we found that the wavelength of the absorbance maximum changed with an increase in the $AgNO_3$ concentration both with and without DNA. Figure 5 shows the changes in the wavelength of the absorbance maximum of the plasmon resonance of silver nanoparticles. With an increase in the silver nitrate concentration, the absorption maximum is shifted to shorter wavelengths; for example, a change in the $AgNO_3$ concentration from 10^{-6} to 10^{-5} M induces a blue shift in the absorbance maximum (λ_{max}) of about 15 nm, that is, the size of nanoparticles increases upon reduction in a concentrated solution of $AgNO_3$.

The influence of DNA on the formation of silver nanoparticles can be clarified by comparing Figures 3 and 4. Although solutions with and without DNA show a very similar general trend in spectral changes, we noted the following differences. (i) The surface plasmon absorbance intensity of silver nanoparticles in solutions with DNA is lower than that in solutions without DNA. (ii) At a silver nitrate concentration of 10^{-4} M, the spectra in solutions with and without DNA are quite different; in a solution without DNA, the symmetry of the plasmon peak is distorted and a shoulder appears at longer wavelengths, while in a solution with DNA, the symmetry of the absorbance peak is preserved. (iii) The wavelength of the absorbance maximum in a solution with DNA is always about 5 nm shorter than that in the same solution without DNA (Figure 5).

Therefore, in good agreement with earlier reports on the stabilizing effect of polymers, DNA, even at a concentration as low as 10^{-8} M, has a stabilizing effect toward silver nanoparticle growth, which is observed by UV−vis spectroscopy as a reduction in nanoparticles size and a narrowing of their size distribution. One possible explanation for this phenomenon may be the physical contact of the polymer chain with the surface of nanoparticles, which prevents its further growth and controls its final size.[17]

In addition to spectroscopic evidence, nanoparticles of transition metals can be directly visualized by TEM. First, we performed TEM observations of samples prepared by mixing $AgNO_3$ and $NaBH_4$ solutions without DNA. Electron micrographs of the silver nanoparticles that formed after reduction at $AgNO_3$ concentrations of 10^{-5} M and 10^{-4} M are shown in Figure 6. The nanoparticles that formed after silver nitrate reduction in 10^{-4} M solution were quite monodisperse, with an average size of about 15 nm. Larger and more monodisperse silver particles were observed at a lower concentration of $AgNO_3$ (10^{-5} M). The size of the observed nanoparticles and the tendency of a size decrease at a higher concentration of silver nitrate are in a good agreement with the spectroscopic observations. We also performed TEM observations of silver nanoparticles in the presence of T4 DNA molecules. Electron micrographs in Figure 7A,A' show silver nanoparticles on a single unfolded DNA chain. Because a giant chain of T4 DNA

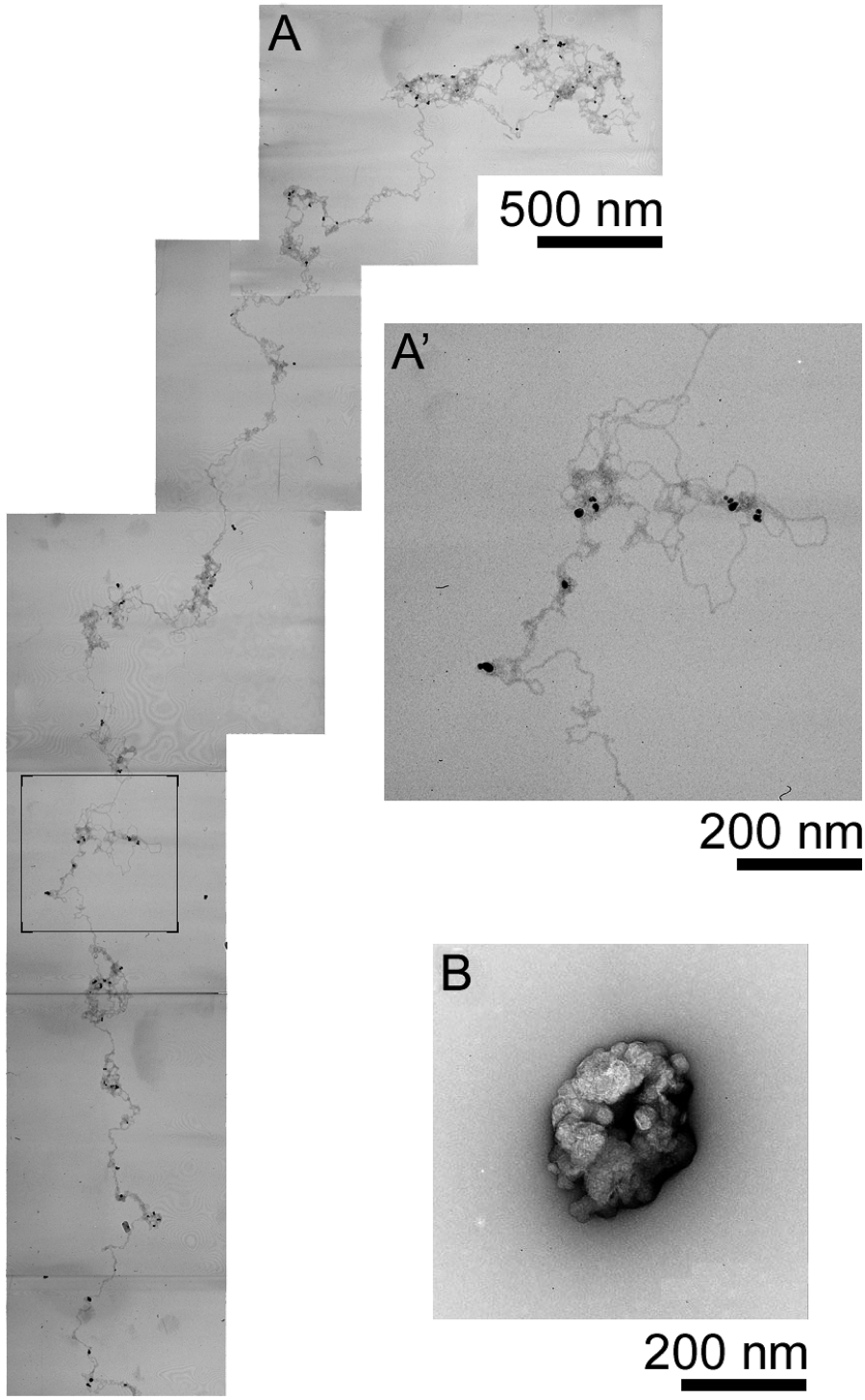

Figure 7. (A) TEM micrographs of T4 DNA interacting with silver nanoparticles formed as a result of $AgNO_3$ reduction by $NaBH_4$. Sample was prepared by the reduction of $AgNO_3$ (10^{-5} M) by $NaBH_4$ (10^{-4} M) in water (Milli-Q) and the final addition of T4 DNA (10^{-6} M). (A') The enlarged part in micrograph A. (B) TEM micrograph of T4 DNA collapsed by silver nanoparticles formed as a result of $AgNO_3$ reduction by $NaBH_4$. Samples were prepared by the reduction of $AgNO_3$ (10^{-5} M) by $NaBH_4$ (10^{-4} M) in water (Milli-Q) and the final addition of T4 DNA (10^{-6} M in nucleotides).

is very long (contour length of about 57 μm), only part of the chain is shown in micrograph A (image height is ca. 7 μm). Black dots on this image correspond to silver nanoparticles, which are mainly associated with DNA chains and are about 15 nm in size.

Figure 7B shows the structure of DNA compacted by reduced silver. The collapsed DNA chain dimension is dramatically smaller than that of unfolded T4 DNA. The DNA condensate has a clear metallic aspect and consists of many discrete units with a nanoparticle-like shape, and thus, such discreteness can only be due to the incorporation of silver nanoparticles into the DNA condensate. Another indication that DNA is incorporated into complex with nanoparticles can be obtained by comparing the size of a DNA condensate with the usual size of a T4 DNA condensate compacted, for instance, by multications. A nanoparticles-compacted DNA condensate (200 nm) is more than twice as large as multication-collapsed DNA (70−100 nm),[18] which indicates the incorporation of nanoparticles into the DNA condensate.

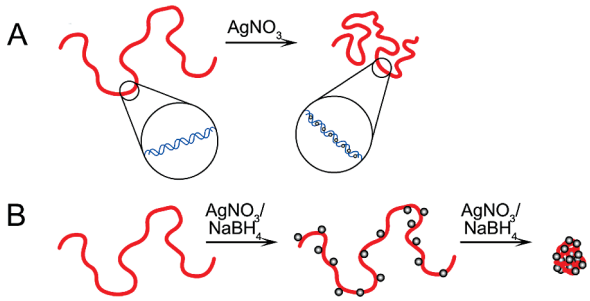

Figure 8. Schematic representation of changes in the conformation of a DNA chain. (A) With the addition of $AgNO_3$, the DNA persistence length decreases, but DNA remains in the coil state. (B) Silver nanoparticles are generated upon $AgNO_3$ reduction with $NaBH_4$ and induce compaction of a DNA chain into a condensate incorporating nanoparticles.

Finally, we performed experiments at different concentrations of DNA and found that in solutions with a higher DNA concentration (10^{-7} M), the concentration of silver ions required for DNA compaction after reduction was several times greater, which indicates that there should be more nanoparticles for a higher total charge of DNA in solution.

The combination of TEM, FM, and spectroscopy methods shows that reduction of silver ion induces DNA compaction. It is generally accepted that the driving force of DNA compaction is neutralization of the total negative charge of DNA.[19] At the pure electrostatic level, it is known that DNA compaction by counterions is mediated by DNA charge neutralization greater than 88−89%.[20,21] Thus, monovalent counterions, such as Ag^+, that induce 76% of charge neutralization of DNA, cannot compact DNA according to Manning-Oosawa condensation theory.[22,23] In contrast, reduction of ionic silver in the DNA solution leads to the DNA compaction. It should be mentioned that metal complexing properties of polyphosphates reported a few decades ago[24] indicate that DNA can behave similarly to polymeric template and, upon reduction of the silver ion, nucleation and growth of nanoparticles take place on a DNA template, which further aggregates into compact condensate. Thus, our experiments show that even without specific cationic modifications of the nanoparticle surface, which has been employed earlier to enable electrostatic interaction with DNA,[25,26] DNA compaction can be readily realized simply by silver reduction to nanoparticles.

The observed mechanism of DNA compaction by $AgNO_3$/$NaBH_4$ is very different from that induced by multivalent cations. According to a well-established model,[27] the mechanism of DNA compaction by low-molecular-weight multications is an all-or-none process, that is, individual chains of DNA undergo a first-order phase transition from the coil into the globule conformation without any intermediate stages. In contrast, DNA collapse induced by silver nanoparticles proceeds by a different scenario: the effective molecular volume of DNA gradually decreases until DNA assumes a compact globule conformation. The formation of multiglobule network aggregates of DNA can be a result of further aggregation of DNA−silver nanoparticle species into larger structures containing several compact DNAs.

Due to the complexity of the DNA/$AgNO_3$/$NaBH_4$ system, several parameters can dramatically influence the efficiency of DNA compaction. For instance, size of silver nanoparticles and the ratio between $AgNO_3$ and $NaBH_4$ are important parameters, which are responsible for the potential of DNA compaction. Detailed investigations on the DNA-compaction activity of the $AgNO_3$/$NaBH_4$ system, depending on different factors such as charge, geometrical properties of Ag nanoparticles, or ionic strength, are currently underway.

Conclusion

Our main conclusions are presented in Figure 8, which shows two cases of changes in the conformation of DNA in silver-containing solutions. We have demonstrated that in a solution of $AgNO_3$ there are no significant changes in the conformational behavior of the double-stranded DNA chain and only shrinking of a DNA coil is noted at high concentrations of Ag^+ due to a decrease in the persistence length of DNA. In contrast, the reduction of $AgNO_3$ by $NaBH_4$ and formation of silver nanoparticles causes DNA compaction into compact globular metallic nanostructures driven by aggregation of silver nanoparticles on DNA chains.

Acknowledgment. This work is partly supported by Grant-in-Aid for Young Scientists No. 18719001 and Grant-in-Aid for Scientific Research in Priority Area No. 20034025 from MEXT, Japan.

References and Notes

(1) Yamane, T.; Davidson, N. *J. Am. Chem. Soc.* **1961**, *83*, 2599–2607.
(2) Yamane, T.; Davidson, N. *Biochim. Biophys. Acta* **1962**, *55*, 609–621.
(3) Jensen, R. H.; Davidson, N. *Biopolymers* **1966**, *4*, 17–32.
(4) DiRico, D. E.; Keller, P. B.; Hartman, K. A. *Nucleic Acids Res.* **1985**, *13*, 251–260.
(5) Izatt, R. E.; Christensen, J. J.; Ryting, J. H. *Chem. Rev.* **1971**, *71*, 439–481.
(6) See, for example: (a) Alivisatos, P. *Science* **1996**, *271*, 933–937. (b) Nie, S.; Emory, S. R. *Science* **1997**, *275*, 1102–1106. (c) Nicewarner-Peña, S. R.; Freeman, R. G.; Reiss, B. D.; He L; Peña, D. J.; Walton, I. D.; Cromer, R.; Keating, C. D.; Natan, M. J. *Science* **2001**, *294*, 137–141. (d) Maier, S. A.; Brongersma, M. L.; Kik, P. G.; Meltzer, S. G.; Requicha, A. A.; Atwater, H. A. *Adv. Mater.* **2001**, *13*, 1501–1505. (e) Kamat, P. V. *J. Phys. Chem. B* **2002**, *106*, 7729–7744. (f) Murray, C. B.; Sun, S.; Doyle, H.; Betley, T. *Mater. Res. Soc. Bull.* **2001**, *26*, 985–991. (g) Alivisatos, A. P.; Barbara, P. F.; Castleman, A. W.; Chang, J.; Dixon, D. A.; Klein, M. L.; McLendon, G. L.; Miller, J. S.; Ratner, M. A.; Rossky, P. J.; Stupp, S. I.; Thompson, M. E. *Adv. Mater.* **1998**, *10*, 1297–1336. (h) Empedocles, S. A.; Neuhauser, R.; Bawendi, M. G. *Nature* **1999**, *399*, 126–130. (i) Zinchenko, A. A.; Yoshikawa, K.; Baigl, D. *Adv. Mater.* **2005**, *17*, 2820–2823.
(7) See, for example: (a) Braun, E.; Eichen, Y.; Sivan, U.; Ben-Yoseph, G. *Nature* **1998**, *391*, 775–778. (b) Richter, J.; Mertig, M.; Pompe, W.; Mönch, I.; Schackert, H. K. *Appl. Phys. Lett.* **2001**, *78*, 536–538. (c) Ford, W. E.; Harnack, O.; Yasuda, A.; Wessels, J. M. *Adv. Mater.* **2001**, *13*, 1793–1797. (d) Mertig, M.; Ciacchi, L. C.; Seidel, R.; Pompe, W.; Vita, A. D. *Nano Lett.* **2002**, *2*, 841–844. (e) Nakao, H.; Shiigi, Y.; Yamamoto, S.; Tokonami, T.; Nagaoka, S.; Sugiyama, S.; Ohtani, T. *Nano Lett.* **2003**, *3*, 1391–1394. (f) Ongaro, A.; Griffin, F.; Nagle, L.; Iacopino, D.; Eritja, R.; Fitzmaurice, D. *Adv. Mater.* **2004**, *16*, 1799–1803. (g) Becerril, H. A.; Stoltenberg, R. M.; Monson, C. F.; Woolley, A. T. *Mater. Chem.* **2004**, *14*, 611–616. (h) Wang, G.; Murray, R. W. *Nano Lett.* **2004**, *4*, 95–10. (i) Nyamjav, D.; Kinsella, J. M.; Ivanisevic, A. *Appl. Phys. Lett.* **2005**, *86*, 093107. (j) Niemeyer, C. M.; Simon, U. *Eur. J. Inorg. Chem.* **2005**, *18*, 3641–3655. (k) Braun, G.; Inagaki, K.; Estabrook, R. A.; Wood, D. K.; Levy, E.; Cleland, A. N.; Strouse, G. F.; Reich, N. O. *Langmuir* **2005**, *21*, 10699–10701. (l) Nyamjav, D.; Kinsella, J. M.; Ivanisevic, A. *Appl. Phys. Lett.* **2005**, *86*, 093107. (m) Wei, G.; Zhou, H.; Liu, Z.; Song, Y.; Wang, L.; Sun, L.; Li, Z. *J. Phys. Chem. B* **2005**, *109*, 8738.
(8) Tsumoto, K.; Luckel, F.; Yoshikawa, K. *Biophys. Chem.* **2003**, *106*, 23–29.
(9) James T. H. *The Theory of the Photographic Process*, 4th ed.; Macmillan: New York, 1977; p 9.
(10) Menzer, S. *J. Am. Chem. Soc.* **1992**, *114*, 4644–4649.
(11) Norden, B.; Matsuoka, Y.; Kurucsev, T. *Biopolymers* **1986**, *25*, 1531–1545.
(12) Makita, N.; Ullner, M.; Yoshikawa, K. *Macromolecules* **2007**, *39* (18), 6200–6206.

(13) Linnert, T.; Mulvaney, P.; Henglein, A.; Weller, H. *J. Am. Chem. Soc.* **1990**, *112*, 4657–4666.
(14) (a) Van Hyning, D. L.; Zukoski, C. F. *Langmuir* **1998**, *14*, 7034–7046. (b) Nickel, U.; Castell, A.; Pöppl, K.; Shirtcliffe, N. *Langmuir* **2000**, *16*, 9087–9091. (c) He, S.; Yao, J.; Jiang, P.; Shi, D.; Zhang, H.; Xie, S.; Pang, S.; Gao, H. *Langmuir* **2001**, *17*, 1571–1575. (d) He, R.; Qian, X.; Yin, Y.; Zhu, Z. *J. Mater. Chem.* **2002**, *12*, 3783–3786. (e) Rodríguez-Gattorno, G.; Díaz, D.; Rendón, L.; Hernández-Segura, G. O. *J. Phys. Chem. B* **2002**, *106*, 2482–2487. (f) Leopold, N.; Lendl, B. *J. Phys. Chem. B* **2003**, *107*, 5723–5727. (g) Velikov, K. P.; Zegeres, G. E.; van Blaaderen, A. *Langmuir* **2003**, *19*, 1384–1389. (h) Tan, Y.; Dai, X.; Li, Y. *J. Mater. Chem.* **2003**, *13*, 1069–1075. (i) Caswell, K. K.; Bender, C. M.; Murphy, C. J. *Nano Lett.* **2003**, *3*, 667–669. (j) Li, X.; Zhang, J.; Xu, W.; Jia, H.; Wang, X.; Yang, B.; Zhao, B.; Li, B.; Ozaki, Y. *Langmuir* **2003**, *19*, 4285–4290.
(15) Mulvaney, P. *Langmuir* **1996**, *12* (3), 788–800, and references cited therein.
(16) Mie, G. *Ann. Phys.* **1908**, *25*, 377–444.
(17) Pastoriza-Santos, I.; Liz-Marzán, L. M. *Langmuir* **2002**, *18*, 2888–2894.
(18) Conwell, C. C.; Vilfan, I. D.; Hud, N. V. *Proc. Natl. Acad. Sci. U.S.A.* **2003**, *100*, 9296–9301.
(19) Bloomfield, V. A. *Curr. Opin. Struct. Biol.* **1996**, *6*, 334–341.
(20) Wilson, R. W.; Bloomfield, V. A. *Biochemistry* **1979**, *18*, 2192–2196.
(21) Baigl, D.; Yoshikawa, K. *Biophys. J.* **2005**, *88*, 3486–3493.
(22) Manning, G. S. *J. Chem. Phys.* **1969**, *51*, 924–938.
(23) Oosawa F. *Polyelectrolytes*; Marcel Dekker: New York, 1971.
(24) Van Wazer, J. R.; Callis, C. F. *Chem. Rev.* **1958**, *58*, 1011–1046.
(25) Ganguli, M.; Babu, J. V.; Maiti, S. *Langmuir* **2004**, *20*, 5165–5170.
(26) Torimoto, T.; Yamashita, M.; Kowabata, S.; Sakata, T.; Mori, H.; Yoneyama, H. *J. Phys. Chem. B* **1999**, *103*, 8799–8803.
(27) Yoshikawa, K.; Takahashi, M.; Vasilevskaya, V. V.; Khokhlov, A. R. *Phys. Rev. Lett.* **1996**, *76*, 3029–3031.

BM800235J